JOURNAL OF MATERIALS SCIENCE 25 (1990) 3142–3148

Superplasticity in an Ni_3Al base alloy with 8 wt % Cr

ASHOK CHOUDHURY, AMIYA K. MUKHERJEE
Division of Materials Science and Engineering, Department of Mechanical Engineering, University of California, Davis, CA 95616 USA.

VINOD K. SIKKA
Metals and Ceramics Division, Oak Ridge National Laboratory, Oak Ridge, TN 37831 USA.

A maximum superplastic elongation of 638% has been obtained in a fine-grained Ni_3Al-based intermetallic alloy containing 8wt% Cr. The extent of superplasticity obtained is dependent on the heat treatment given to the alloy, the test temperature and the strain rate. The activation energy of deformation and the value for the strain rate sensitivity parameter were comparable to those noted earlier in metallurgical alloy systems. There was some evidence that dynamic recrystallization plays a role in determining the extent of cavitation in the grain sized encountered here.

1. Introduction

Significant improvements in the room temperature ductility of substoichiometric (with respect to Al) Ni_3Al have been achieved by careful control of alloy stoichiometry and microalloying with boron [1, 2]. At high temperature however, the alloy is susceptible to a form of intergranular brittleness known as dynamic embrittlement [3, 4]. This occurs under the simultaneous action of oxygen and a high enough temperature and stress level. It has also been found that the addition of about 8 wt % Cr to the alloy significantly alleviates this problem [5]. In so doing, however, about 5 to 15% of the disordered f.c.c. gamma phase is introduced in this otherwise single phase (Gamma Prime) ordered structure ($L1_2$). This alloy has been named IC 218 at the Oak Ridge National Laboratory.

In the course of investigating the high temperature tensile behaviour of IC 218, it was found that given an appropriate thermomechanical treatment to obtain a fine grain size, the alloy could be rendered superplastic. This paper reports the results obtained from tensile tests carried out under different regimes of strain rates and temperatures. The results from the mechanical tests are correlated with microstructural information and fractographic features.

2. Experimental procedure

The chemical composition of the cast and wrought material used in this study is given in Table I. The alloy was thermomechanically processed to yield 0.762 mm thick sheet with a fine grain size. Tensile specimens were punched out from these sheets such that the gauge length was 25.4 mm while the gauge width was 3.175 mm. Specimens were annealed in two batches in air. One batch was annealed for 1 h at 1 050° C (hereafter called HT1) while another batch was annealed for 2 h at 1 150° C (hereafter called HT2).

Following the annealing treatment, specimens were tensile tested in air in the temperature range of 25° C to 1100° C. The testing was done in an instron machine run in the constant extension rate mode. The majority of tests were carried out at an extension rate of 0.021 mm sec^{-1} (0.05 in min^{-1}). Extension rates of 2.12×10^{-3}, 0.212 and 0.423 mm sec^{-1} (0.005, 0.5 and 1.0 in min^{-1}, respectively) were also tried on single specimens. Since the gauge length of the specimens was 25.4 mm, the initial strain rates corresponding to the above mentioned extension rates are 8.3×10^{-4}, 8.3×10^{-5}; 8.3×10^{-3} and 1.7×10^{-2} sec^{-1}, respectively. Testing conditions will henceforth be referred to in terms of these initial strain rates.

Fractographic observations were made on selected specimens using an SEM. Standard metallographic techniques were also used to study the optical microstructure of selected specimens at regions close to the fracture tip.

3. Results and discussions

Table II shows the test conditions and results (*Note: Engineering values*) of all the mechanical tests conducted in this investigation. Fig. 1 is a montage of the HT1 samples tested at an extension rate of 8.3×10^{-4} sec^{-1} obtained after testing at various temperatures.

TABLE I Chemical composition (wt %) of IC 218 alloy used in this study

Al–8.5
Cr–7.8
Zr–0.8
B–0.02
Ni–Bal.

0022–2461/90 $03.00 + .12

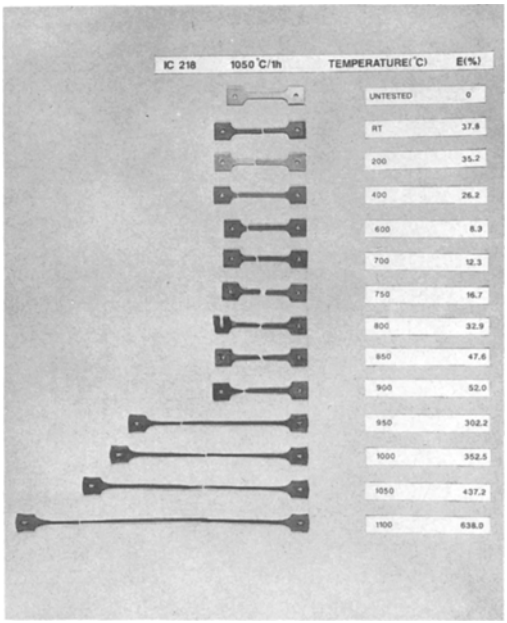

Figure 1 Montage of HT_1 samples tested at the temperatures indicated. All specimens were tensile tested at a confident extension rate with an initial strain rate of 8.3×10^{-4} sec^{-1}.

The effect of heat treatment on the temperature dependence of the 0.2% offset yield strength and the ultimate tensile stress (UTS) is shown in Figs 2a and b, respectively. Two aspects are immediately obvious; (a) while the UTS shows a continuous decrease with increasing temperature, the yield strength is virtually insensitive to temperature until a temperature of about 800° C is reached whereupon the yield strength shows a rather drastic decrease with further increase in temperature, (b) while the HT1 samples are slightly stronger at lower temperatures, above 800° C the HT2 samples are stronger. It is expected that the HT1 specimens will have a grain size somewhat smaller than the HT2 specimens. It is thus not surprising that

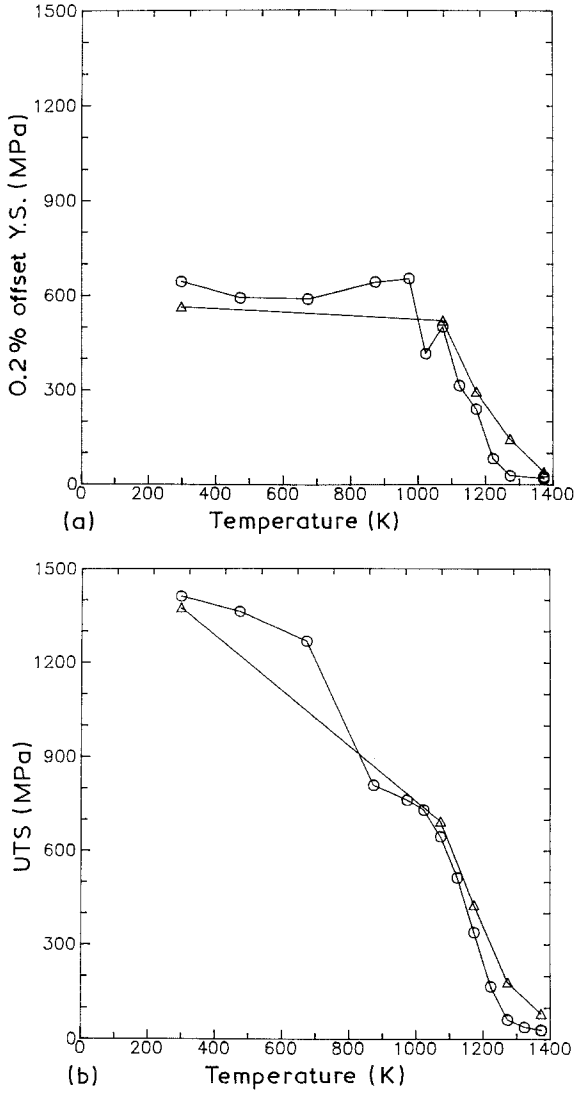

Figure 2 (a) Effect of heat treatment on the temperature dependence of the 0.2% offset yield strength. (b) Effect of heat treatment on the temperature dependence of the UTS. (○) ANN/1050/1H, (△) ANN/1150/2H.

TABLE II Test conditions used and results of tensile tests obtained in this study

Spec #	Strain Rate (sec^{-1})	HT	Temp. (K)	Y.S. (MPa)	UTS (MPa)	Elong. (%)	R.A. (%)
1L	8.3×10^{-4}	HT1	298	643.45	1410.34	37.78	25.12
16L	8.3×10^{-4}	HT1	473	591.72	1360.69	35.18	22.57
17L	8.3×10^{-4}	HT1	673	588.28	1264.83	40.19	26.20
18L	8.3×10^{-4}	HT1	873	642.76	806.28	8.27	8.68
12L	8.3×10^{-4}	HT1	973	653.79	760.69	12.31	13.97
13L	8.3×10^{-4}	HT1	1023	415.86	729.66	16.73	13.13
14L	8.3×10^{-4}	HT1	1073	502.07	644.14	32.92	45.31
2L	8.3×10^{-4}	HT1	1123	314.48	512.41	47.62	94.38
3L	8.3×10^{-4}	HT1	1173	240	337.93	51.98	91.19
10L	8.3×10^{-5}	HT1	1173	35.17	87.59	226	87.97
4L	8.3×10^{-4}	HT1	1223	82.07	166.21	302.17	81.05
5L	8.3×10^{-4}	HT1	1273	28.28	61.38	352.50	64.52
6L	8.3×10^{-4}	HT1	1323		37.93	437.20	91.63
7L	8.3×10^{-3}	HT1	1323		151.03	109.23	91.05
11L	1.7×10^{-2}	HT1	1323		224.14	190.52	91.722
15L	8.3×10^{-4}	HT1	1373	19.31	28.28	638.15	88.12
20L	8.3×10^{-4}	HT1	1373	25.52	29.66	469.12	86.98
21L	8.3×10^{-4}	HT2	298	563.45	1373.45	38.12	26.34
22L	8.3×10^{-4}	HT2	1073	520.69	693.10	10.09	4.87
23L	8.3×10^{-4}	HT2	1173	295.17	425.52	38.07	35.22
24L	8.3×10^{-4}	HT2	1273	144.83	179.31	127.62	77.62
25L	8.3×10^{-4}	HT2	1373	39.31	80	207.20	84.11

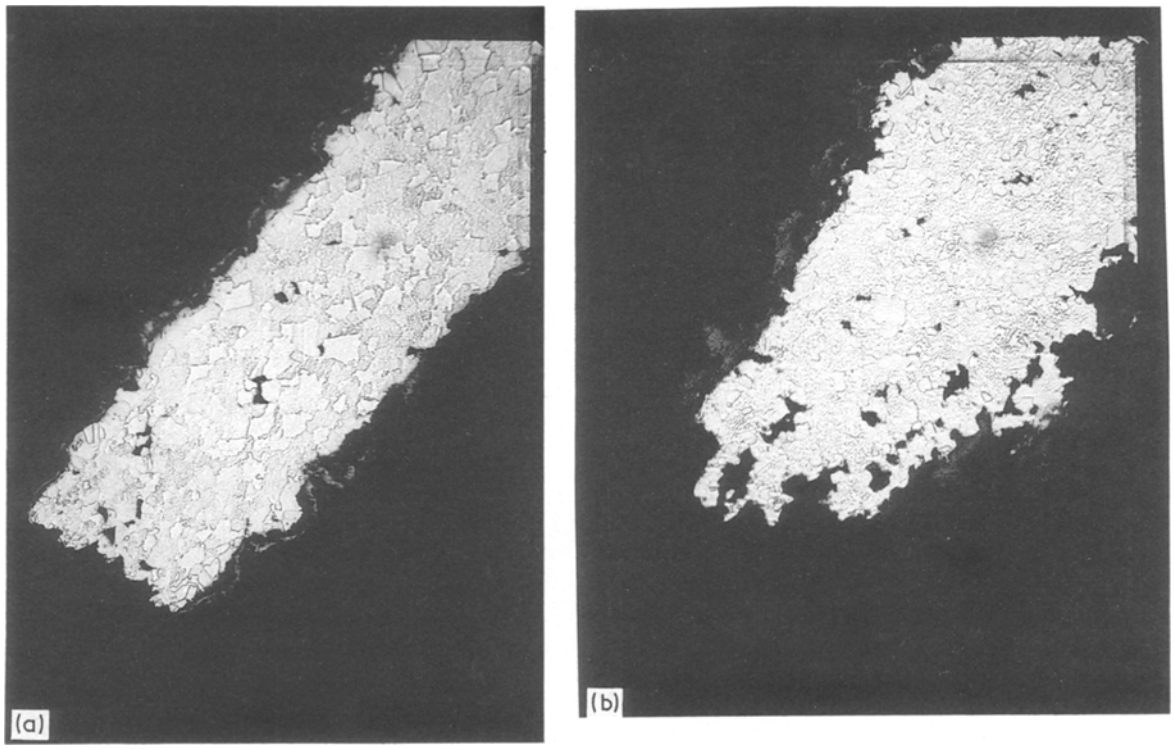

Figure 3 Optical micrographs taken adjacent at the fracture tips for specimens given different heat treatments but tested under similar conditions. (a) Anealed at 1050° C for 1 h. (b) Annealed at 1150° C for 2 h. (× 300 for both figures)

the HT1 specimens have a higher yield strength than the HT2 specimens at the lower temperatures through the Hall-Petch effect. On the onset of grain boundary sliding (around 800° C) however, the situation is reversed and the smaller grained HT1 specimens show a lower yield strength. Figs 3a and b show the effect of heat treatment on the grain size. These optical micrographs were obtained from the heads of specimens 20L and 25L, respectively, after the specimens had been tensile tested to failure at 1 100° C. From these micrographs, specimen 20L has a grain size of about 13 μm after the test, while 25L shows a grain size of about 20 μm. As mentioned in Table II, 20L had been given an HT1 treatment and displayed a ductility of 469% while 25L had been given an HT2 treatment and displayed a ductility of 207%. At the test strain rate of $8.3 \times 10^{-4} \text{sec}^{-1}$, these values translate to test times of approximately 94 min and 41 min for 20L and 25L, respectively. The larger grain size seen for 25L (Fig. 3b) as compared to 20L (Fig. 3a) thus cannot be ascribed to longer residence time at test temperature. This strongly suggests that the HT1 treatment did indeed yield a finer grain size than the HT2 treatment. It is felt that some grain growth did occur during the test; hence, it would seem that a grain size lower than 13 μm would be desirable for obtaining superplasticity in this system.

The dependence of ductility (% elongation and % reduction in area) on heat treatment is shown on Figs 4a and b, respectively. From Fig. 4a it appears that significant ductility (in what would normally be considered the superplastic range) is achieved only beyond

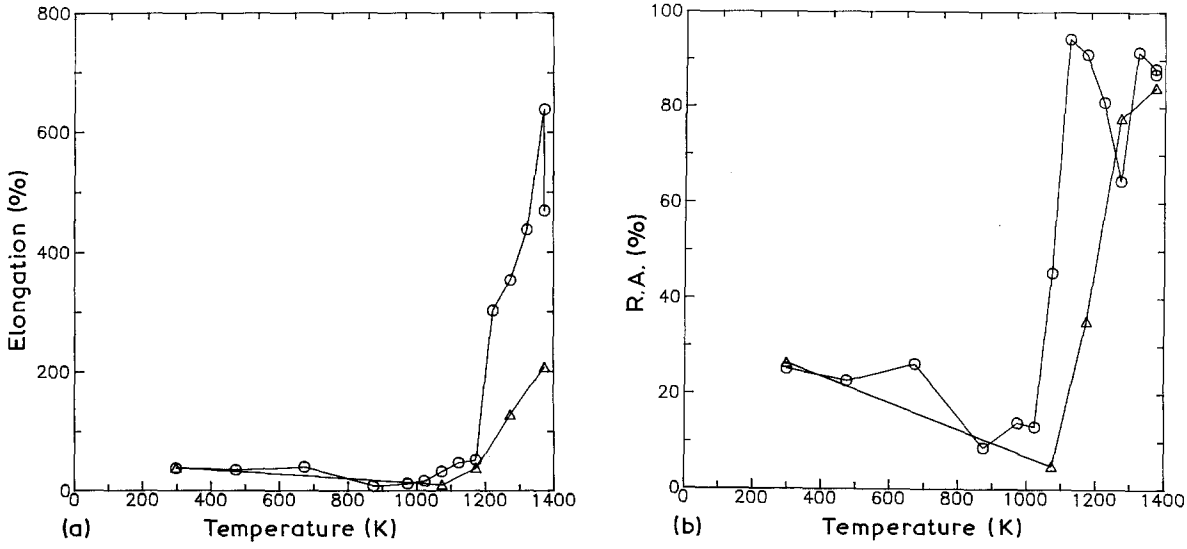

Figure 4 (a) Effect of heat treatment on the temperature dependence of the percentage elongation. (b) Effect of heat treatment on the temperature dependence of the percentage reduction in area. (○) ANN/1050/1H, (△) ANN/1150/2H.

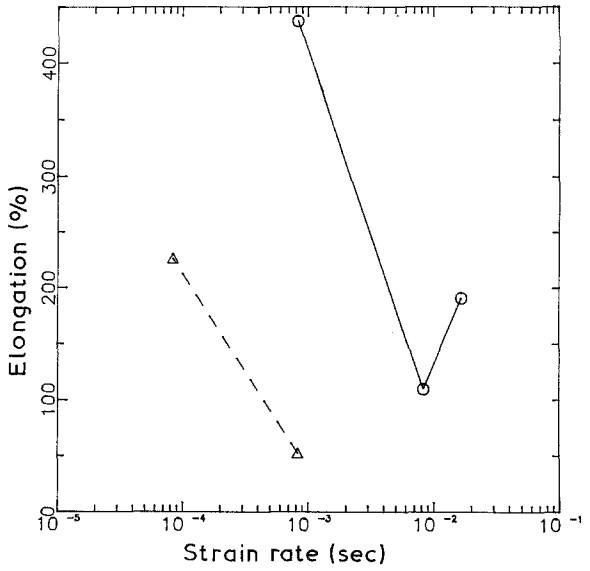

Figure 5 The strain rate dependence of ductility at two temperatures. (○) 1050° C, (△) 900° C.

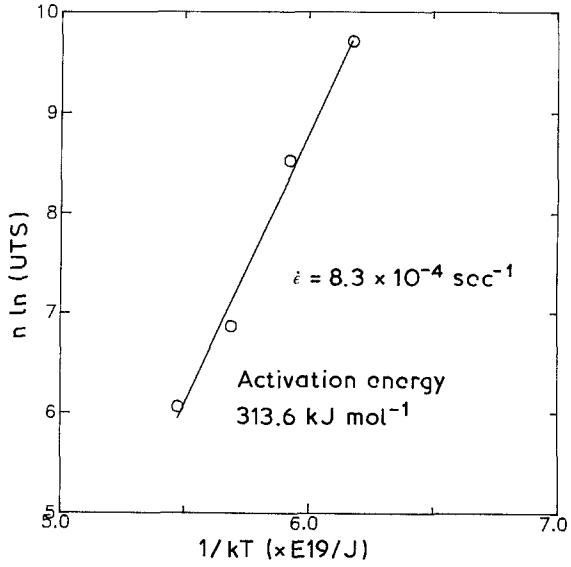

Figure 7 Arrhenius plot of the temperature dependence of the UTS.

900° C. At present we cannot explain the cusp (Fig. 4b) in the % reduction in area between 850° C and 1 050° C. It is to be noted that a maximum elongation of 638% has now been achieved in an alloy that at one time was considered "dead brittle".

It is fairly obvious from the above results that this material exhibits superplastic behaviour. If such is indeed the case, both the strength and the ductility should be strain rate sensitive. In this investigation only the HT1 specimens were tested over a limited range of strain (extension) rates. Fig. 5 shows the dependence of the % elongation at fracture on the strain rate at two temperatures. Note that at the lower temperature (900° C) only two strain rates were studied. An obvious trend is that at a given temperature the ductility decreases with increasing strain rate. Also, the ductility obtained at a given strain rate increases with increasing test temperature. Fig. 6 shows the UTS as a function of strain rate at two temperatures. It appears that the slopes are identical at the two temperatures although only two data points are presented at 900° C. The strain rate sensitivity of the UTS, i.e., the parameter m is found to be 0.6 (the stress exponent is thus 1.66). Using this value of the stress exponent, the Arrhenius plot of the temperature dependence of UTS at a constant strain rate shown on Fig. 7 yields an apparent activation energy for superplastic flow of 313 KJ mole^{-1}. This value is in general agreement with the values found for the activation energy for bulk diffusion in several Ni_3Al-based alloys [6, 7, 8, 9, 10].

The fracture surfaces of specimens 20L (HT1) and 25L (HT2) are compared in Figs 8a and b, respectively. Both SEM fractographs show intergranular

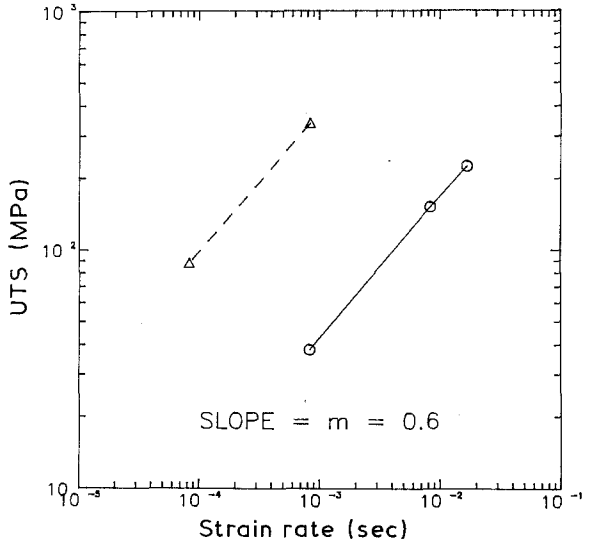

Figure 6 The strain rate dependence of the UTS at two temperatures. (○) 1050° C, (△) 900° C.

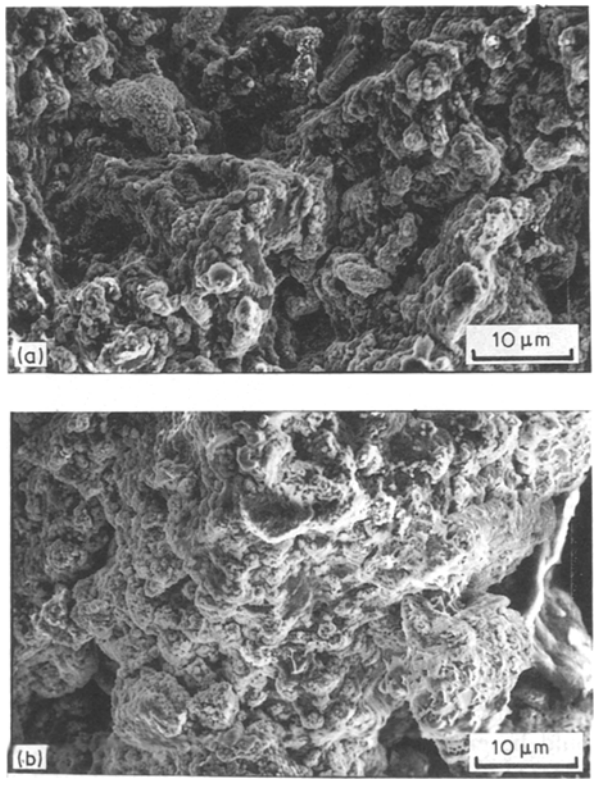

Figure 8 SEM fractographs of samples given different heat treatments but tested under similar conditions (1 100° C, $\dot{\varepsilon} = 8.3 \times 10^{-4}$ sec^{-1} (a) Annealed at 1 050° C for 1 h, (b) annealed at 1 150° C for 2 h.

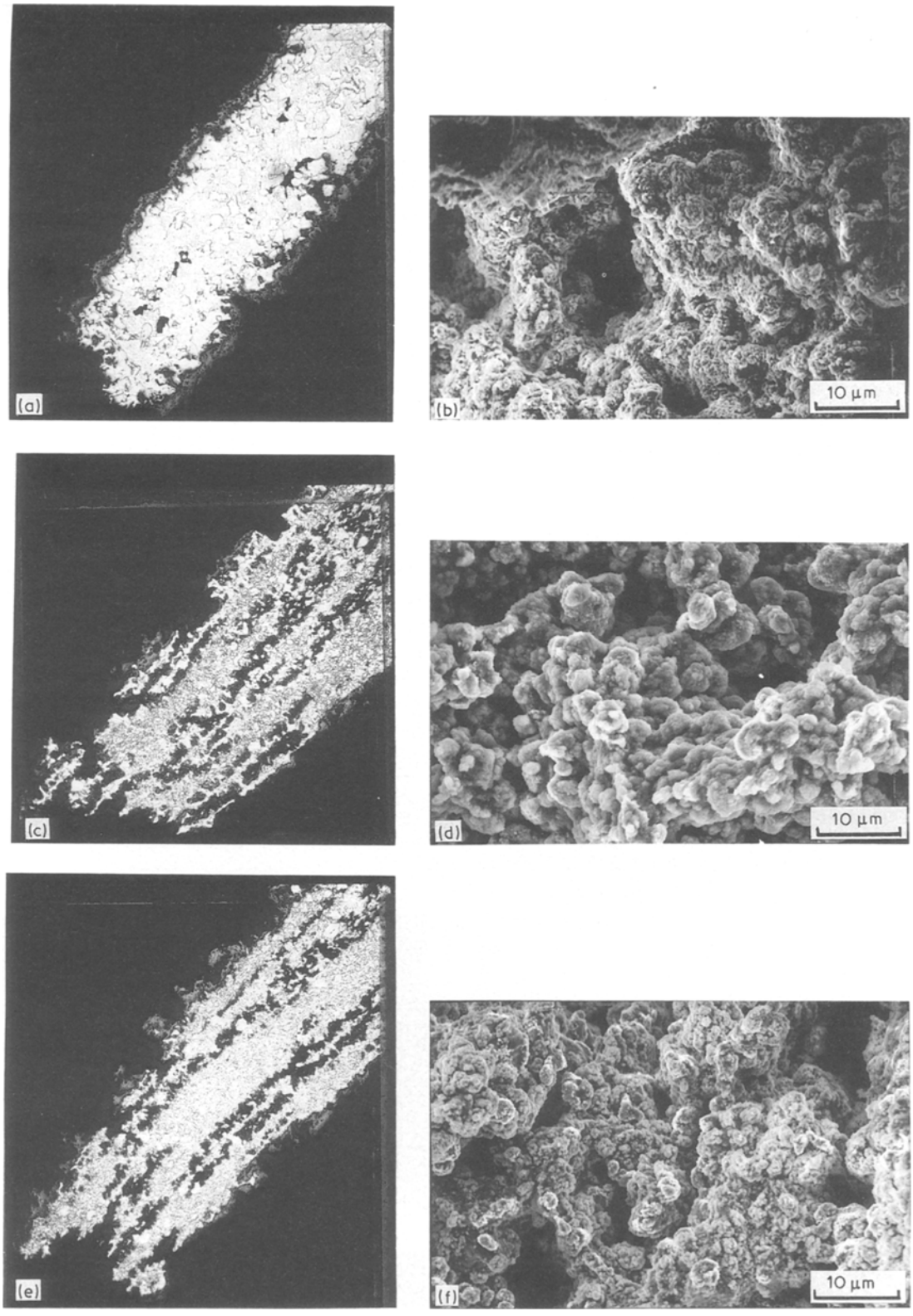

Figure 9 Montage of optical micrographs (a, c and e, all at 300 ×) and SEM fractographs (b, d and f) showing the effect of strain rate on level of cavitation and the ensuring fracture morphology. Strain rates for Figs a and b is 8.3×10^{-4} sec^{-1}; for Figs c and d, 8.3×10^{-3} sec^{-1} and for Figs e and f, 1.7×10^{-2} sec^{-1}.

features characteristic of high temperature fracture and there does not appear to be any difference between them. The tiny globules seen on both fractographs could be either dynamically recrystallized grains or oxides formed on the fracture surfaces during the high temperature exposure to air following fracture. As mentioned earlier, Figs 3a and b show the optical micrographs of these two specimens close to the fractured tips. It is to be noted that the HT2 specimen (Fig. 3b) shows a significantly higher level of intergranular cavitation than the HT1 specimen (Fig. 3a). This probably accounts for the lower elongation obtained in the former case (Table II). Both specimens however, do show rather fine grains at the fracture tip; these are probably dynamically recrystallized grains formed in the most highly stressed region of the specimens – the fracture location. The present findings are in agreement with the work of Takeyama and Liu [11]

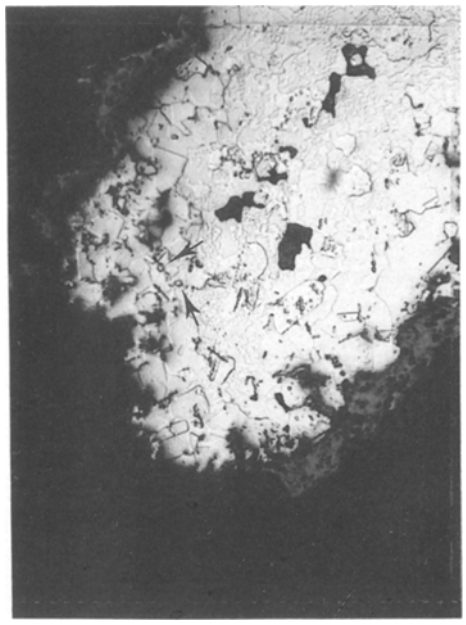

Figure 10 High magnification micrograph at the fracture tip of a specimen (6L) showing evidence (arrowed) of dynamic recrystallization. 390x.

on the effects of grain size and test temperature on the fracture behaviour and ductility of Ni_3Al.

The effect of strain rate on the microstructure and resulting fractographic features are shown on the montage of Fig. 9. All specimens depicted here were given the same heat treatment (HT1) and tested at 1 050° C. The optical micrographs show extensive cavitation at strain rates greater than $8.3 \times 10^{-4}\,sec^{-1}$. It is primarily as a consequence of this that the lowest strain rate specimen displays the highest ductility. It is well known that dynamic recrystallization is one of the mechanisms available for relieving stress concentrations at grain boundaries during high temperature deformation. If the time available at high temperature is not enough to dynamically nucleate new strain-free grains, it is possible to envision a situation where the stress concentrations produced by grain boundary sliding during superplastic deformation is relieved by the formation of cavities. This seems to be the case for the specimens deformed at strain rates of $8.3 \times 10^{-3}\,sec^{-1}$ and $1.7 \times 10^{-2}\,sec^{-1}$. Figure 10 is a high magnification micrograph of the fracture tip of the specimen deformed at a strain rate of $8.3 \times 10^{-4}\,sec^{-1}$. The dynamically recrystallized grains are clearly visible. Baker *et al.* [12], have previously observed dynamic recrystallization in Ni_3Al.

Figs 11a and b show the optical micrograph and the SEM fractograph respectively of specimen 16L which was deformed at 200° C at a strain rate of $8.3 \times 10^{-4}\,sec^{-1}$. The heat treatment given to this specimen was the same as for the specimens shown on Fig. 9. The optical micrographs of Fig. 9, however, do not show the distinct banded structure evident in Fig. 11a. This implies that the HT1 treatment was insufficient to wipe out the vestiges of cold rolling. During high temperature testing, however, the combined effect of dynamic recrystallization, grain boundary sliding, grain rotation (confirmed in preliminary studies) and the enhanced rates of diffusion are sufficient to obliterate the residual banded structure. The structure seen after testing these specimens (e.g. Figs 9a, c and e) thus appears equiaxed. The change in fracture morphology from primarily ductile transgranular at low temperatures to primarily intergranular at high temperatures is evident by comparing Fig. 11b with Figs 9b, d and f.

4. Conclusions

1. A maximum elongation of 638% has been obtained in an Ni_3Al – based alloy containing 8 wt % Cr (IC 218). In order to achieve this level of superplastic ductility, it is necessary to use a thermomechanical processing treatment that yields a fine grain size.

2. The extent of superplasticity obtained is dependent on the heat treatment given to the alloy, the test temperature and the strain (extension) rate. For this alloy the optimum superplastic conditions were found at a test temperature of 1 100° C and at an extension rate of $8.3 \times 10^{-4}\,sec^{-1}$ when the alloy was annealed for 1 h at 1 050° C.

3. For the particular alloy studied, the strain rate sensitivity of the UTS was found to $m = 0.6$. The

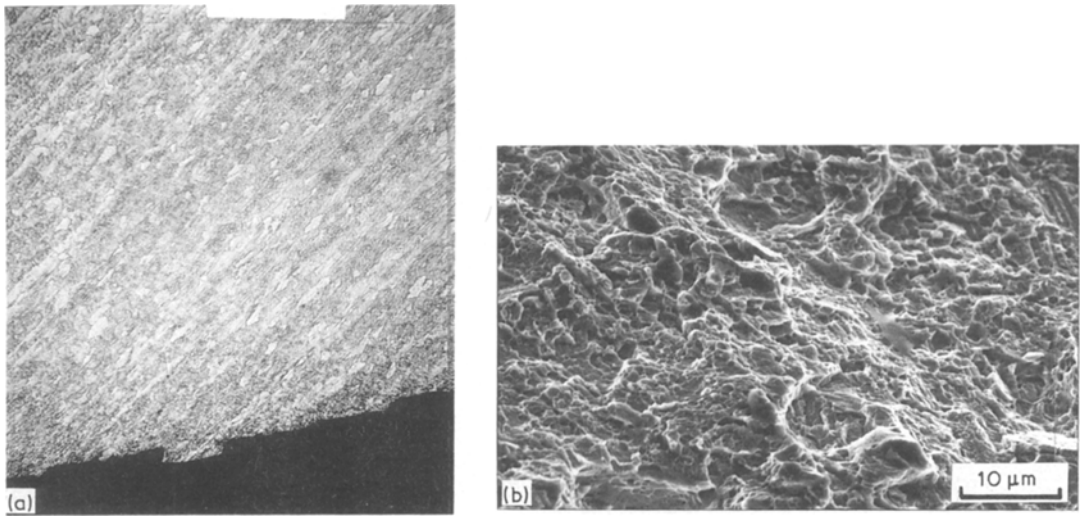

Figure 11 Optical micrograph (a) 195x and SEM fractograph (b) of specimen tested at 200° C at an initial strain rate of $8.3 \times 10^{-4}\,sec^{-1}$. The effect of test temperature is seen by comparing these to Figs 9a and b.

activation energy for superplastic deformation was found to be 313 KJ mole^{-1}. This value compares well with reported values for the activation energy for bulk diffusion in this class of alloys.

4. Metallographic evidence suggests that dynamic recrystallization plays a significant role in determining the extent of cavitation in this alloy. This in turn can control the maximum obtainable elongation at fracture.

5. As anticipated, the fracture morphology changes from a predominantly transgranular nature at low temperature to a predominantly intergranular type at elevated temperature.

References

1. K. AOKI and O. IZUMI, *Nippon Kinzoku Gakkaishi,* **43 (12)** (1979) 1190–1195.
2. C. T. LIU, C. L. WHITE and J. A. HORTON, *Acta Metall.* **33 (2)** (1985) 213–229.
3. C. T. LIU and C. L. WHITE, *Acta Metall.* **35 (3)** (1987) 643–649.
4. C. T. LIU, "High Temperature Ordered Intermetallic Alloys II" in MRS Symposium Proceedings, Boston, Massachusetts, **Vol. 81**. Edited by N. S. Stoloff, C. C. Koch, C. T. Liu and O. Izumi, (1987) pp. 355–367.
5. C. T. LIU and V. K. SIKKA, *J. Metals* **38** (1986) 19–21.
6. J. H. SCHNEIBEL, G. F. PETERSON and C. T. LIU, *J. Mater. Res.* **1 (1)** (1986) 68–72.
7. T. C. CHOU and Y. T. CHOU, "High Temperature Ordered Intermetallic Alloys I", MRS Symposium Proceedings, Boston, Massachusetts, **Vol. 39**. Edited by C. C. Koch, C. T. Liu and N. S. Stoloff, (1985) pp. 461–474.
8. P. A. FLINN, *Trans. TMS-AIME,* **218** (1960) 145–154.
9. J. R. NICHOLLS and R. D. RAWLINGS, *J. Mater. Sci.* **12** (1977) 2456–2464.
10. K. HOSHINO, S. J. ROTHMAN and R. S. AVERBACK, *Acta Metall,* **36 (5)** (1988) 1271–1279.
11. M. TAKEYAMA and C. T. LIU, *Acta Metall.* **36 (5)** (1988) 1241–1249.
12. I. BAKER, D. V. VIENS and E. M. SCHULSON, *Scripta Metall.* **18 (3)** (1984) 237–240.

Received 31 January
and accepted 24 August 1989